APOE, Immune Factors, Sex, and Diet Interact to Shape Brain Networks in Mouse Models of Aging

Steven Winter[1], Ali Mahzarnia[2], Robert J Anderson[2], Zay Yar Han[2], Jessica Tremblay[2], Daniel Marcellino[3], David B. Dunson[1], Alexandra Badea[2,4,5,*]

*Corresponding author

Alexandra Badea, PhD

Alexandra.badea@duke.edu

[1]Statistical Science, Trinity School, Duke University, Durham, NC, USA

[2]Department of Radiology, Duke University School of Medicine. Durham, NC, USA

[3]Department of Integrative Biology, Umea University, Sweden

[4]Department of Neurology, Duke University School of Medicine. Durham, NC, USA

[5]Duke UNC Brain Imaging and Analysis Center, Duke University School of Medicine. Durham, NC, USA

Abstract

The exact mechanisms through which the APOE gene influences Alzheimers disease risk (AD) are under intense investigation. Yet, much remains unknown about how APOE alleles interact with age, sex, and diet to confer vulnerability to select brain networks. To address this question, we used mouse models that carry the three major human APOE alleles, and have a mouse like, or humanized innate immune system. This was realized through the replacement of the mouse with the human inducible nitric oxide synthase (iNOS) gene, leading to a lower immune response. Our study combines advanced, accelerated diffusion imaging methods with novel statistical analyses to reveal global and local brain graph differences, associated with each of the following risk factors for abnormal aging and AD: age, APOE genotype, sex, diet, innate immune response. We used a sparse logistic regression model (GraphClass) with complimentary pairs stability selection to identify small and robust subnetworks predictive of individual risk factors. The comparison of APOE3 versus APOE4 carriage identified 773 edges, with no more than 40 false selections; age resulted in 300 high selection probability edges with <5 false selections, sex resulted in 540 high selection probability edges with <7 false selections; diet in 1626 high selection probability edges with <31 false selections; and humanizing NOS in 411 edges with <9 false selections. Our results revealed widespread network differences due to age and diet, including the temporal association cortex, and also regions involved in response to threatening stimuli, such as the amygdala and periaqueductal gray. Sex associated differences affected regions such as the thalamus, insula and hypothalamus, but also fimbria and septum, involved in memory processes. APOE genotype was associated with differences in the connectivity of memory related areas, and also in sensory and motor areas; while diet and innate immunity (HN) were associated with differences in insula and hypothalamus connectivity. We pooled these models to identify common networks across multiple traits, giving insight into shared vulnerability amongst the risk factors. We identified 63 edges out of the total 54,946 edges (0.11% of the connectome) as common to all risk factors tested. Our results revealed common subnetworks vulnerable to several risk factors for AD, in an approach that can provide new biomarkers, and targets for therapies.

Keywords: APOE, LOAD, connectomics, MRI, diffusion, Alzheimer's disease

1. Introduction

Alzheimer's disease (AD) affects 6.7 million Americans, and takes a huge toll on the elderly and the society in general, yet we still do not have a full understanding of the factors and mechanisms conducive to its development. The vast majority of AD patients suffer from late onset AD (LOAD). Of the known risk genes for LOAD, APOE has been shown to have the strongest impact (Corder, Saunders et al. 1993)(Raber, Huang et al. 2004) (Liu, Liu et al. 2013). Among its three common allelic isoforms, APOE4 confers the greatest genetic risk for AD, APOE3 is neutral, and APOE2 is thought to confer protection. While the percentage of APOE4 carriers is ~25 %, they represent ~ 65% of the LOAD patients in US (Mayeux, Saunders et al. 1998) (Ward, Crean et al. 2012). Old age is the major unmodifiable risk factor, and >13% of people over 75 are affected by LOAD (TheAlzheimer' sAssociation 2023). Other unmodifiable risk factors include a family history of Alzheimer's disease, and female sex, with 2/3 of LOAD patients being women. It is unclear how APOE genotype interacts with sex, to increase risk in females (Raber, Wong et al. 1998). Modifiable risk factors for developing Alzheimer's disease include a history of brain injuries in males, diabetes, hypertension, and obesity in middle age (Chuang, An et al. 2016, Singh-Manoux, Dugravot et al. 2018) (Hersi, Irvine et al. 2017). Understanding the role of these factors can help devise strategies for successful aging.

While historically research efforts have been centered on the role of hippocampus and the entorhinal cortex as early markers of neurodegeneration, the field of connectomics has switched the perspective towards studying networks. Brain networks are sensitive to small alterations due to multiple factors leading to disease, and enable the propagation of pathology. Such alterations are not uniform across the cortex, and the timing and pattern of local changes may inform on vulnerable regions and their inter-relationships, as captured in connectomes (Filippi, Cividini et al. 2023). Assessing network based differences across the life span or due to interventions, stressors, risk factors can inform on disease etiology, progression and response therapeutic treatments. Importantly, structural brain changes may occur decades before overt disease manifestation, and detecting such changed early will help identify individuals at risk, and novel targets for therapies. Connectome differences have been detected for various conditions in human populations (Mitra, Shen et al. 2016, Verhelst, Vander Linden et al. 2018, Kuceyeski, Jamison et al. 2019; Mahzarnia, Stout et al. 2023), and also in animal models (Badea,

Kamnaksh et al. 2018) (Wang, Bey et al. 2016, Wang, Anderson et al. 2018, Badea, Ng et al. 2019). Most human research has been concerned with restructuring of functional networks, but an investigation of structural networks and the interplay of these two can reveal novel insight into the biological substrates for brain changes during aging (Zamani Esfahlani, Faskowitz et al. 2022), and AD. For example, reduced coupling between functional and structural connectomes has been observed in sensory motor regions during aging, but it was preserved for areas of higher cognitive function (Zamani Esfahlani, Faskowitz et al. 2022). Detecting differences early on, in individuals at risk or in animal models of risk, is thus a worthwhile direction for future research.

Our study focuses on how APOE, as a genetic risk factor modulating cardiovascular and brain risk, confers vulnerability to select brain networks. While APOE4 may confer certain advantages early in life, it is known to increase risk during aging. Thus, understanding the dynamics of connectomes along the age span, in relation to genetic and other risk factors has been a topic of great interest (Dennis, Browndyke et al. 2010, Brown, Terashima et al. 2011, Trachtenberg, Filippini et al. 2012, Xie and He 2012, Veitch, Weiner et al. 2019). While the idea that APOE4 carriers suffer from accelerated aging has been proposed multiple times, and specific diets and exercise interventions have been proposed to curb the risk for age related diseases, we still need to better understand the APOE interaction with female sex, diet and the immune system.

One way to address such knowledge gaps is to use mouse models, since they reach “old age” faster than humans, and can model genetic risk for AD, through targeted replacement of the mouse Apoe gene with the three major human isoforms. These models have been used to reveal alterations in functional connectivity, associated with cerebral perfusion (Valerio, Maximilian et al. 2014), and how it can be affected by diet (Wiesmann, Zerbi et al. 2016). Furthermore, behavioral and imaging studies have examined phenotypic changes in the presence of different APOE human isoforms (Raber, Huang et al. 2004) (Badea, Wu et al. 2019). In this work we used mouse models with APOE2, APOE3 and APOE4 alleles, conferring different levels of risk for AD (Xu, Schmechel et al. 1996, Sullivan, Mezdour et al. 1997), and crossed them with mouse models with a humanized innate immune system, where the mouse Nos2 gene has been replaced with the human NOS2 gene (Colton, Vitek et al. 2006, Colton, Wilcock et al. 2008). We used high-resolution diffusion imaging to construct structural connectomes. Our goal was to examine how unmodifiable and modifiable risk factors including APOE, age, and

sex, as well as a high fat diet confer selective vulnerability to brain networks. In addition, we investigated whether humanizing the innate system modifies the network structure of the brain in aged animals. Finally, we identified brain networks that were vulnerable to multiple risk factors.

2. Methods

2.1 Animals

All animal procedures were approved by the Duke Institutional Animal Care and Use Committee. To model genetic risk for aging and Alzheimer's disease, we used targeted replacement mice lacking the mouse Apoe gene, and homozygous for the human APOE2, APOE3, and APOE4 alleles, instead of the mouse Apoe genes (Xu, Schmechel et al. 1996, Sullivan, Mezdour et al. 1997). The animals were donated by Dr Nobuyo Maeda and maintained in the Duke colony. To better mimic the human innate immune system, we crossed these animals with mouse mice lacking the mouse Nos2, and expressing the human NOS gene. As a result, these mouse models have a more human like innate immune system. These HuNOS2tg/mNos2$^{-/-}$ mice, termed HN, were donated by Dr Colton. The NOS2 gene manipulation has been linked to oxidative processes and response, DNA repair, and mitochondrial activity, altering TNFα and Ccr1 mRNA expression in the HN mice compared to WT (Colton, Vitek et al. 2006, Colton, Wilcock et al. 2008). The humanized APOE lines were crossed with the HN mice until homozygous for each of the three APOE alleles, double KO for mNos2 and expressing humanized NOS. Both males and females were included, for a total of 173 mice ranging from 13 to 20 months of age; their genotype and sex distribution are shown in Table 1.

	Male	High Fat Diet	Above Group Median Age	HN	Total
APOE2	16	15	23	25	59
APOE3	11	26	12	22	58
APOE4	16	15	16	29	58

Table 1: Genotype and sex distribution of mouse models.

Group median ages were calculated separately for basic and HN lines, as 16.2 and 15.2 months.

Animals were bred as homozygous for each of the APOE alleles, to completely lack the mNos2, and to express hNOS2. These animals were aged naturally, and were either maintained on a regular chow (2001 Lab Diet) for the whole duration, or switched for 4 months prior to imaging to a high fat diet (D12451i, Research Diets) containing 45 kcal % fat (39 kcal % from lard; 5 kcal % from oil), 35 kcal % carb (17 kcal % sucrose), and 20 kcal % protein for approximately 4 months. In contrast control diet animals received 13.6 kcal % fat, 57.5 kcal carb (3.25 sucrose), and 28.9 kcal % protein throughout their life span. Animals had free access to food and water. The mean of each age category were 14.60±1.13 months, and 19.35±1.59 respectively; while the median age was16.2. Animals were sacrificed during a transcardiac perfusion fixation under surgical plane anesthesia with 100 mg/Kg ketamine and 10 mg/Kg xylazine, before being perfused through the left cardiac ventricle, with outflow from the right atrium. Saline (0.9%) was used to flush out the blood, at a rate of 8 ml/min for ~5 min. For fixation we used a 10% solution of neutral buffered formalin phosphate containing 10% (50 mM) Gadoteridol (ProHance, Bracco Diagnostics Inc., Monroe Township, NJ, United States), at a rate of 8 ml/min for ~5 min. Gadoteridol reduced the spin lattice relaxation time (T1) of tissue to ~100 ms. Mouse heads were trimmed of extraneous tissue, and stored in 10% formalin for 12 h, then transferred to a 0.01 M solution of phosphate buffered saline (PBS) containing 0.5% (2.5 mM) Gadoteridol, at 4°C for ~30 days to rehydrate the tissue. Specimens were placed in MRI-compatible tubes, immersed in perfluoropolyether (Galden Pro, Solvay, NJ, United States) for susceptibility matching. Specimens were left inside the skull to preserve tissue integrity and shape, but extraneous muscles tissue and lower jaw were removed to allow close positioning in a tight fitting solenoid coil.

2.2 Image Acquisition and Processing

Diffusion weighted magnetic resonance imaging was done using a 9.4T high field MRI, with a 3D SE sequence with TR/TE: 100 ms/14.2 ms; matrix: 420 × 256 × 256; FOV: 18.9 mm × 11.5 mm × 11.5 mm, 45 μm isotropic resolution, BW 62.5 kHz; using 46 diffusion directions, 2 diffusion shells (23 at 2,000, and 23 at 4,000 s/mm^2); 5 non-diffusion weighted (b0), as in Badea, Li et al. (2022). The max diffusion pulse amplitude was 130.57 Gauss/cm; duration 4 ms; separation 6 ms, eightfold compressed-sensing acceleration (Tamir, Ong et al. 2016, Anderson, N. Wang et al. 2018). Diffusion tensor properties such as fractional anisotropy, orientation distribution

functions, and tractograms were reconstructed and SIFT filtered using MRtrix3 (Tournier, Smith et al. 2019). We used pipelines implemented in a high-performance computing environment (Anderson, Wang et al. 2018) to segment the brain in 332 sub regions, from which we have excluded cerebrospinal fluid to reconstruct connectomes as adjacency matrices, where each entry represented the number of streamlines connecting a pair of brain regions. The connectome generation pipeline is available at https://github.com/Ali-Mahzarnia/Connectome_tracts_pipeline.

2.3 Statistical Analysis

2.3.1 Exploratory Analysis

Many previous studies have identified relationships between brain topology and traits. As a first step for our analyses, we selected common topological summary statistics (eigenvector centrality, betweenness centrality, global efficiency, local efficiency, average clustering, degree, shortest path length, and degree Pearson correlation) and used t-tests to study the differences in means for each statistic across trait levels. False discoveries were controlled with FDR adjusted p-values (FDR =0.05).

2.3.2 Sparse Network Regression

We fit seven sparse logistic regression models, predicting APOE2/APOE3, APOE3/APOE4, APOE2/APOE4, mNos/hNOS, below/above median age, female/male, and regular/high-fat diet from vectorized connectomes. Selected edges from each model (i.e., entries of vectorized connectomes with nonzero coefficients) were pooled into subnetworks that are predictive of each trait.

The sparse logistic regression models used the GraphClass double sparsity penalty defined in Arroyo Relión, Kessler et al. (2019). Let B be a 332x332 symmetric matrix of coefficients, with b_{ij} the coefficient for the edge between regions i and j in a logistic regression model. Let $B_{(v)}$ be the vth row (or column) of B, v=1,…,332. The GraphClass penalty is:

$$\lambda\left(\rho\|B\|_1+\sum_{v=1}^{332}\|B_{(v)}\|_2\right)$$

where $\lambda, \rho > 0$ are sparsity hyperparameters. The first term, $\|B\|_1$, is the usual Lasso penalty and shrinks the coefficients of each edge towards zero. The second term, $\|B_{(v)}\|_2$, penalizes the coefficients of all edges connected to region v. In practice, this effectively deletes entire regions from the connectome, resulting in sparser and more interpretable subnetworks. The penalized model is fit with the alternating direction method of multipliers (ADMM). Hyperparameters were selected via 10-fold cross-validation minimizing missclassification rate, and ties were broken by selecting the sparsest model.

2.3.3 Stability Selection

A subnetwork selected by a single run of GraphClass may be unreliable due to noise in the data and high correlation between entries of the connectomes. Following Arroyo Relión, Kessler et al. (2019), we used complimentary pairs stability selection (CPSS, Shah and Samworth (2013)) to improve the robustness and reliability of our analysis. CPSS is based on the intuition that truly important edges will be selected in a very high fraction of repeated experiments (e.g., selecting new mice, reproducing the study, and fitting GraphClass), whereas less important edges will be selected in a low portion of repeated experiments. Resampling techniques can be used to estimate the selection frequency of each edge across many synthetic experiments, resulting in an estimate of high selection probability (HSP, present in >99% of experiments) and low selection probability (LSP) edges. Theoretical bounds on the number of LSP edges falsely labeled as HSP edges are available under weak conditions. We used this procedure with defaults from Shah and Samworth (2013) to identify small, reliable subnetworks with false-selection guarantees.

2.3.4 Subnetwork Ranking

In general, HSP subnetworks will have many disjoint connected components. In order to make the results more interpretable, we propose a rule for ranking the relative importance of connected components within each HSP network. This is achieved by comparing the Bayesian Information Criterion (BIC) of unpenalized logistic regression models predicting the trait using only the edges in a single connected component. BIC balances predictive performance and model complexity, allowing for fair comparisons between subnetworks of different sizes. We consider connected components with lower BIC to be more important for explaining a trait than those with higher BIC.

2.3.5 Validation

GraphClass and stability selection produce seven subnetworks for predicting each of APOE2/APOE3, APOE3/APOE4, APOE2/APOE4, mNos/hNOS, below/above median age, female/male, and regular/high-fat diet. We validated these subnetworks using AUC/ROC. AUC/ROC was computed by fitting GraphClass regression on half of the samples, using only edges in the HSP subnetwork. This model was used to predict class labels for the other half of the samples. The entire procedure was repeated 10 times with different train/test splits.

2.3.6 Common Networks

We define the shared high selection probability (HSP) network across multiple models as the intersection of the HSP networks for each model. For example, the shared networks across age and APOE3/APOE4 contains all the edges that are in the HSP network for age and also in the HSP network for APOE3/APOE4; edges that are only in the HSP network for age or only in the HSP network for APOE3/APOE4 are not included.

3. Results

3.1 Group-level Differences in Network Parameters Differentiate with Risk Factors for LOAD

We first performed an exploratory data analysis to reveal global differences for key network parameters. **Table 2** shows FDR-corrected p-values from t-tests for differences in topological summaries between groups.
Multiple tests were significant after FDR correction. Brain networks above/below median age had significant differences in eigenvector/betweenness centrality, local efficiency, average clustering, and shortest path length, suggesting broad differences in connectivity, information flow, and resilience. No tests were significant for groups with different diets. Local efficiency and shortest path length varied significantly with sex, suggesting innate differences in resilience and information flow. All measures except local efficiency and degree Pearson correlation were significantly different between mNOS and hNOS, indicating strong differences in connectivity, information flow, and resilience.

	Age	Diet	Sex	mNos/hNOS	APOE2-3	APOE2-4	APOE3-4
Eigenvector centrality	0.0017**	0.78	0.58	0.039*	$1.8x10^{-5}$**	0.29	0.03*
Betweenness centrality	0.78	0.073	0.45	0.017*	$2.9x10^{-7}$**	$3.5x10^{-5}$**	0.073
Global efficiency	0.20	0.69	0.38	0.0063*	0.24	0.75	0.36
Local efficiency	0.044*	0.79	0.022*	0.38	0.20	0.72	0.36
Average clustering	0.0037**	0.10	0.31	$2.0x10^{-6}$**	0.039*	0.75	0.20
Degree	0.20	0.66	0.36	0.0056*	0.24	0.75	0.36
Shortest path length	0.0053*	0.40	0.022*	0.022*	0.9	0.24	0.14
Degree Pearson correlation	0.72	0.78	0.66	0.91	$1.45x10^{-5}$**	0.0009**	0.38

Table 2: FDR corrected p-values for t-tests comparing topological summary statistics (*p<0.05, **p<0.005).

All pairwise APOE comparisons had significant differences in eigenvector and/or betweenness centrality, suggesting strong differences in connectivity. Average clustering was significant only for APOE3/APOE3. Interestingly, the degree Pearson coefficient was only significant for APOE genotype comparisons, in particular for APOE2/APOE3, and APOE2/APOE4, highlighting variations in brain network assortativity for the APOE2 genotype.

3.2 Vulnerable Subnetworks Associated with Risk Factors for LOAD

We identified subgraphs discriminating amongst mouse models with different risk factors for AD, including genotype, age, sex, diet, and immune background. For simplicity, we visualize only the top 50 edges (by

coefficient magnitude) within each HSP subnetwork. The false selection bounds still apply to this subpopulation of edges.

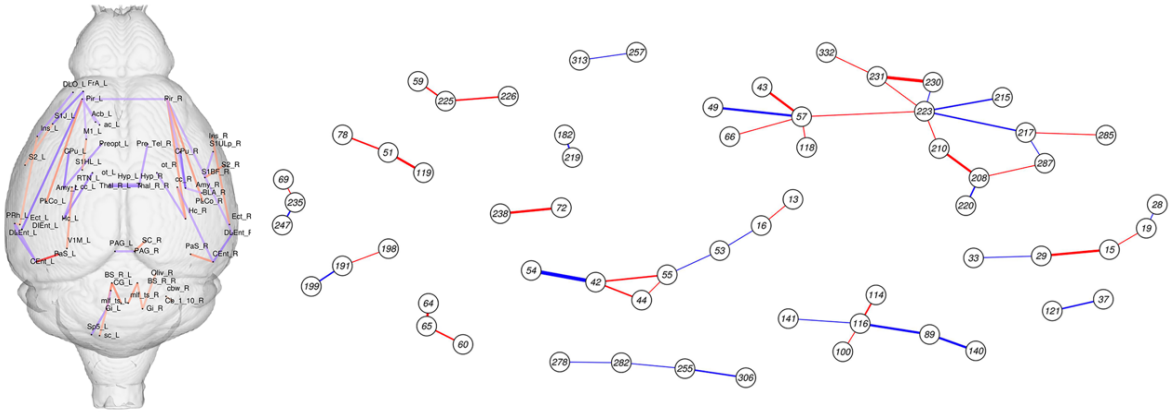

A: APOE2 versus APOE3

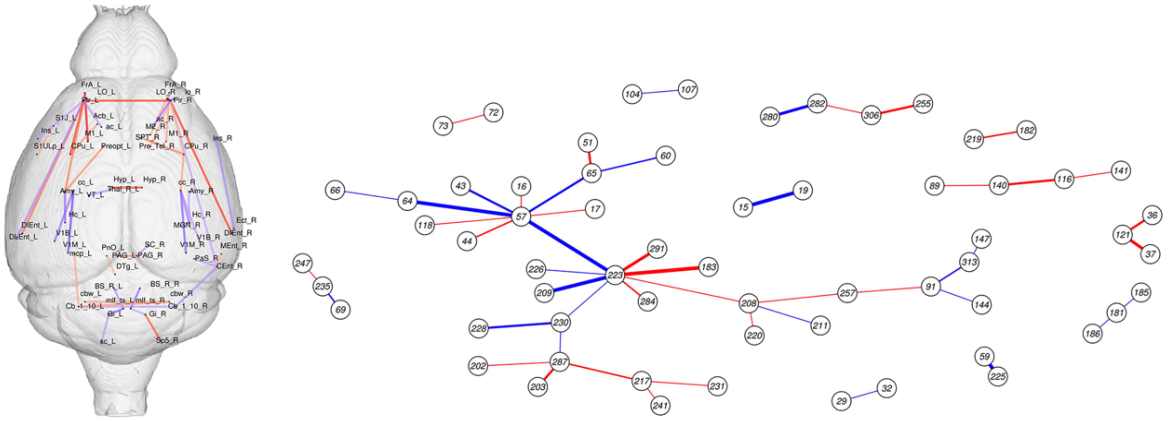

B: APOE3 versus APOE4

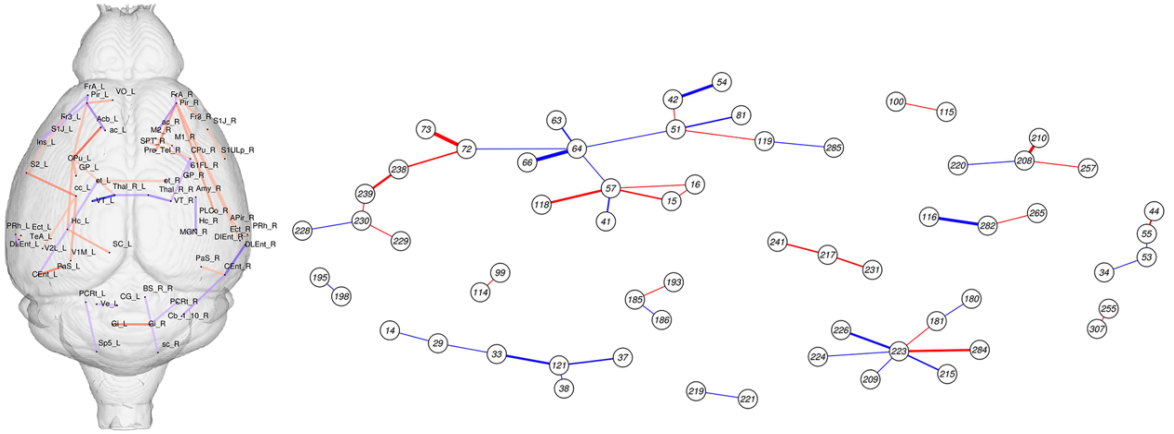

C: APOE2 versus APOE4

Figure 1: Subgraphs discriminating with APOE genotype. A. APOE2 versus APOE3; B. APOE3 versus APOE4; C. APOE2 versus APOE4. We noted a central role for the caudomedial entorhinal cortex, cortical

amygdaloid nucleus, and piriform cortex (nodes 42, 49, 57) for the APOE2/APOE3 comparison (A); the frontal association cortex, M1, piriform cortex (L, and R), and striatum (nodes 15, 19, 57 , 223 and 64) for APOE3/APOE4 (B); the striatum, accumbens, caudomedial entorhinal cortex, parasubiculum, and the gigantocellular reticular nucleus (nodes 64, 66, 42, 54, 116 and 282) for APOE2/APOE4. Red denotes positive, blue denotes negative edge weights.

APOE2/APOE3: When comparing connectomes of APOE2 versus APOE3 mice we identified a total of 273 nonzero edges with <8 false selections, pinpointing networks possibly associated with resilience. To aid with interpretability, we then decimated the subgraphs based on edge associated weight values to preserve the top 50 nodes **(Figure 1A).** The lowest BIC (107.4) was associated with a subnetwork that included 7 regions: the dorsolateral orbital cortex, caudomedial and dorsolateral entorhinal cortex, insula, ectorhinal cortex, parasubiculum, and perirhinal cortex. Although the weights were higher for the left hemisphere, the contralateral nodes were also represented into the subgraph (**Suppl Table 1**). The second ranked subnetwork (BIC=126.5) included 16 regions, i.e. the entorhinal cortex (dorsolateral and intermediate), bilateral piriform cortex and amygdala (posterior cortical amygdaloid nucleus, basolateral, rest of amygdala), hippocampus and parasubiculum, and striatum, parasubiculum; and from white matter tracts the anterior commissure (Left, or L), corpus callosum (Right,or R), optic tracts (R). The 3rd ranked network (BIC=131.3) included the preoptic telencephalon, striatum and amygdala. Thus, we observed subnetworks considered part of the limbic system, and brain regions related to executive function, memory and sleep.

APOE3/APOE4: When contrasting APOE3 versus APOE4 mice to pinpoint networks associated with vulnerability in APOE4 carriers relative to the control allele we identified a total of 773 nonzero edges with <40 false selections (**Figure 1B**). The models for this case were much less sparse than the previous one, which is reflected in the presence of massive networks and looser false selection bound. The top two networks included the connections between the left frontal association cortex and M1 (BIC=147.5); and the connections between areas of the visual cortex (monocular and binocular V1 areas) and corpus callosum (BIC=148.8). The subsequent ranked subnetworks involved the brain stem, giganotocellular nucleus, trigeminal and tectospinal

tracts; as well as the periaqueductal gray and superior colliculus. We noted a large subgraph (33 regions) including the insula, lateral orbital cortex, entorhinal cortex, piriform cortex, parasubiculum, hippocampus, striatum, amygdala, accumbens, and cerebellum, as well as V1, medial geniculate and cerebellar peduncle, preoptic telencephalon and septum (BIC=156.9). Thus, in addition to the executive, and memory networks observed between APOE2 and APOE3 mice, we observed a sensory motor component when comparing APOE3 and APOE4 mice.

APOE2/APOE4: When comparing connectomes of APOE2 versus APOE4 mice, to compare the effects of the protective versus the risk associated APOE alleles, we identified 204 edges with no more than 4 expected false selections (**Figure 1C**). The first subnetwork was composed of 21 regions (BIC=104.8), i.e. the frontal association cortex, insula, ventral orbital cortex, entorhinal cortex, piriform cortex, septum, parasubiculum and hippocampus, as well as thalamus including ventral thalamic nuclei, striatum and globus pallidus, accumbens, and superior colliculus. The second subnetwork also included the frontal association cortex, frontal cortex area 3, the entorhinal cortex, piriform cortex, amygdala (posterolateral cortical amygdaloid nucleus, and the amygdalapiriform transition area), preoptic telencephalon and anterior commissure. The third network included S1 (forelimb area, M1, and M2). Thus, we have identified subnetworks incorporating regions involved in executive function, memory, as well as sensory motor areas, sleep, and reward processes.

In addition to APOE genetic risk factors, we have examined differences with age, sex, high fat diet, and immune background (**Figure 2**). To address these risk factors, we performed comparisons for two classes at a time for mice at different levels for age, sex, and diet with or without human NOS carriage.

Age: Age (moving from ages smaller to higher than the median age of 15 months) yielded 300 high selection edges with <5 false selections. The top 50 edges are shown in (**Figure 2A)**, and they formed 9 subgraphs. The top subnetworks in increasing order of BIC values included the interhemispheric periaqueductal gray connections involved in responses to threatening stimuli (BIC=211.2); the spinal trigeminal and gigantocellular reticular nuclei (BIC=213.8); the temporal and frontal association cortex, S1, secondary auditory cortex, ectorhinal and perirhinal cortex (BIC=239.4). These results suggest variations in executive function, sensory and motor function, and

response to stressors across the age span. We also noted subnetworks involving hypothalamus, S1, S2, V1, and the pons. The largest HPS subnetwork in this set included 31 regions, e.g. the frontal and temporal association cortex, ventral orbital cortex, S1, S2, entorhinal cortex, olfactory tract, piriform cortex, amygdala, accumbens, globus pallidus and striatum, as well as the cerebellum gray, and also white matter. White matter tracts include the anterior commissure, lateral olfactory tract trigeminal nerve, and corpus callosum. Unsurprisingly, age influenced a large portion of the brain connectome.

Sex. Sex differences (moving from female -> male) resulted in 540 high selection probability edges with no more than 7 false selections (**Figure 2B)**. The top subgraph (BIC=201.4) included the reticular nuclei (parvicellular, principal sensory trigeminal, intermediate), gigantocellular, medial longitudinal fasciculus, tectospinal tract. The 2nd and 3rd subgraphs (BIC=203.2; and 213.5, respectively) included the right (2nd subgraph) and left (3rd subgraph) thalamus, ventral and reticular nuclei, internal capsule, striatum. The corpus callosum was also a component of the 2nd subgraph. Interestingly the 4th component (BIC=215.5) include the entorhinal cortex, parasubiculum, hippocampus and cerebellum. The 8th network included the preoptic telencephalon, hypothalamus, and amygdala. These results support a strong hypothalamic component, and the gigantocellular components supports differences in locomotor recovery after injury (Anne, Flavio et al. 2020).

Control/high-fat diet: A comparison based on diet (high fat to regular diet) identified 1626 high selection probability edges with no more than 31 false selections (**Figure 2C)**. The top subgraph (BIC=193.5) included the periaqueductal gray, superior colliculus, cerebellar cortex, as well as V1, caudomedial entorhinal cortex, hippocampus and amygdala, and the reticular nucleus of thalamus. The 2nd subgraph (BIC=200.25) included the insular, lateral orbital cortex, dorsolateral entorhinal cortex, piriform, septum, preoptic telencephalon, striatum and the lateral olfactory tract. The 3rd and 4th graph related the olivary complex with the rest of the brain stem (BIC=201.5,204.5). The thalamus, hippocampus, and temporal association cortex, and auditory cortex were also found among the nodes of the top subnetworks.

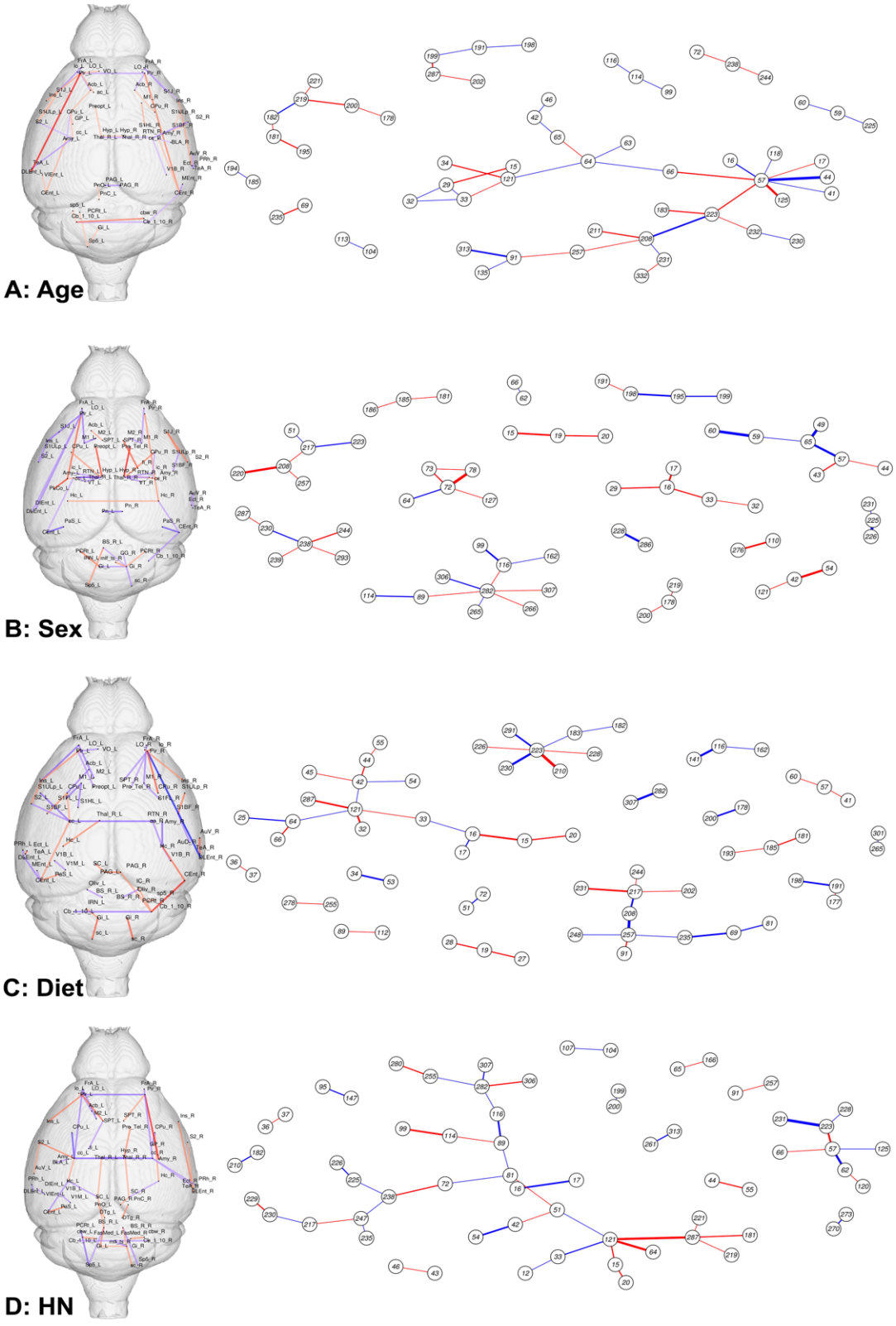

Figure 2: Subgraphs discriminating with age, sex, diet, immune background. A. Age showed nodes a central role for nodes 44, 208, 57, 223 i.e. the dorsolateral and caudomedial entorhinal cortex, piriform cortex (L, and R). B. Sex showed a central role for nodes 59 and 60 the hypothalamus and preoptic telencephalon, and 286

and 228 i.e. fimbria and septum, possibly linking sex vulnerability to memory function. C. Diet showed important roles for regions 121, 223, 230 i.e. corpus callosum and piriform cortex, as well as striatum. D. HN showed a role for nodes 121 and 287 i.e. corpus callosum, as well as 223 and 231 piriform cortex and amygdala. Red denotes positive, blue denotes negative edge weights.

mNos/hNOS: A comparison of hNOS carriage (moving from mNos to hNOS) identified 411 edges with <9 false selections (**Figure 2D)**. The top subgraph (BIC=165.3) was composed of 32 regions, including the secondary auditory cortex, secondary somatosensory cortex and secondary motor cortex, as well as the frontal association cortex, entorhinal and ectorhinal cortices, perirhinal, parasubiculum, hippocampus, thalamus, superior colliculus, striatum, globus pallidus, hypothalamus, preoptic telencephalon, gigantocellular reticular nuclei, periaqueductal gray, and areas of the brain stem plus tracts such as the corpus callosum, spinocerebellar, tectospinal, medial longitudinal fasciculus. The 2nd subgraph (BIC-171.8) included the pirifrom cortex, septum, accumbens, amygdala, fimbria, and the olfactory tract. Interestingly the 3rd and 4th networks included the cerebellar fastigial nucleus, and cerebellar white matter. The insula and entorhinal cortex were found in the next ranked subgraph (BIC=216.8). The pontine reticular nuclei and dorsal tegmentum were present as well in the top ranked subnetworks. Thus, extensive networks were influenced by modification of the immune background.

3.3 Validation

As outlined in Section 2.3.4, we validated the high selection probability subnetworks by predicting each trait with GraphClass using only edges in the selected network. **Figure 3** shows ROC curves with the median AUC across repeated train/test splits. **Table 3** shows the resulting mean AUCs with standard deviations. All models performed very well, despite the extreme sparsity of the selected networks.

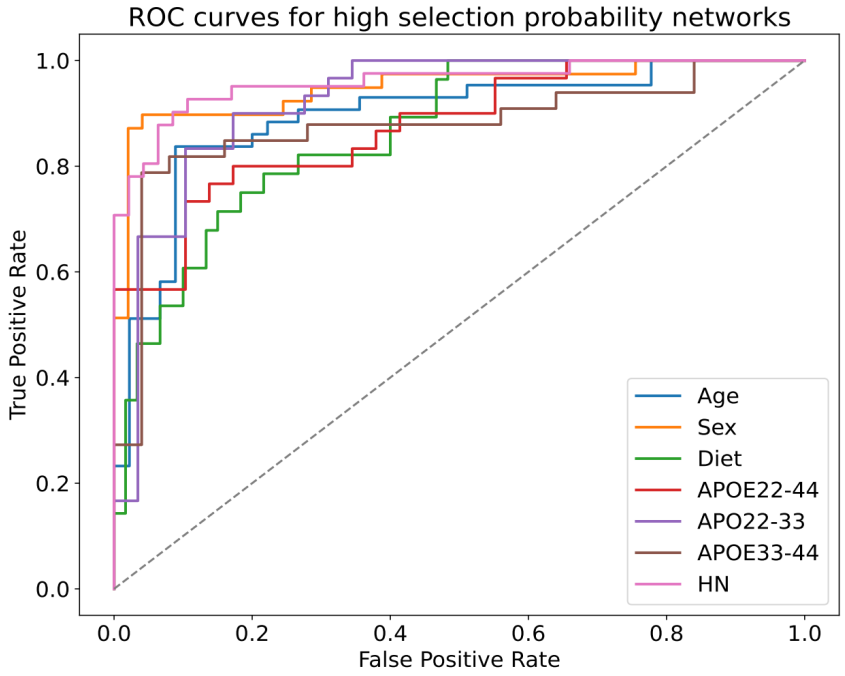

Figure 3: ROC curves with median AUC for all traits.

	Age	Diet	Sex	mNos/hNOS	APOE2-3	APOE2-4	APOE3-4
AUC (std)	0.90 (0.03)	0.86 (0.02)	0.96 (0.03)	0.95 (0.02)	0.92 (0.03)	0.87 (0.03)	0.87 (0.04)

Table 3: Average AUCs and standard deviations across 10 train/test splits.

3.3 Brain Networks with Shared Vulnerability Across Risk Factors for LOAD

We next pooled independent analyses as described in section 2.3.6 to obtain vulnerable brain networks associated with multiple risk factors. These networks are visualized in **Figure 4**, and interpreted below.

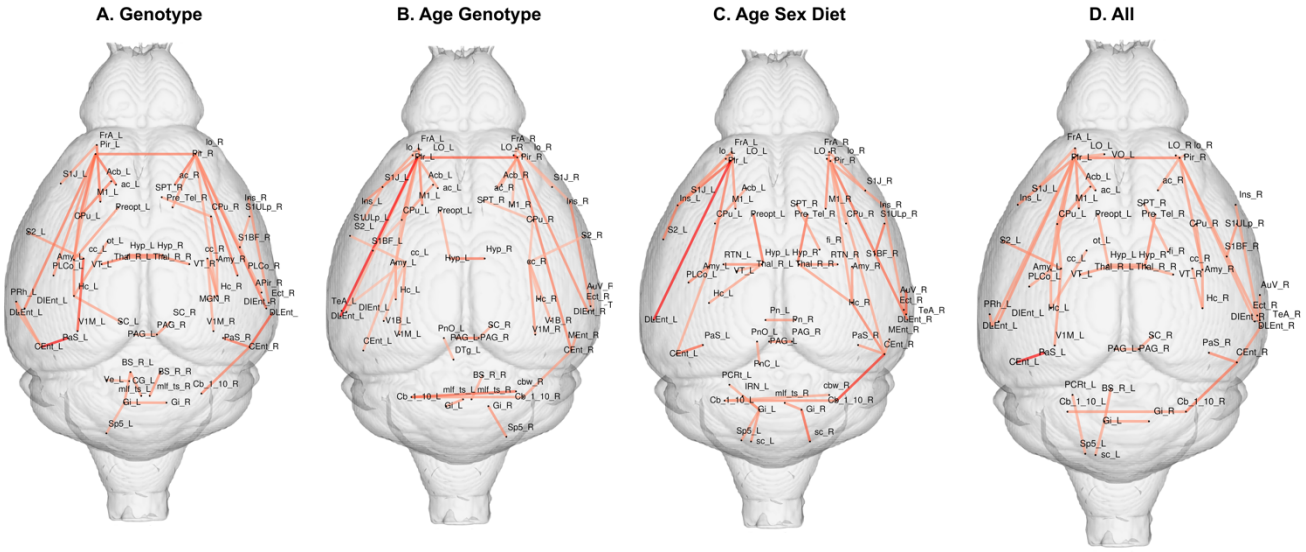

Figure 4. Common edges for vulnerable brain networks associated with distinct risk factors for late onset AD. A. APOE genotype associated networks; B. Age and APOE genotype; C. Age, sex and diet; D. Age, sex, APOE genotype, HN genotype, and diet.

APOE Genotype

We identified 110 edges that were sensitive to variation in APOE genotype for all paired comparisons. These constituted 13 subnetworks and the top 50 edges by cumulative weight across all three HSP networks are shown in **Figure 4 A**. The top subnetwork involved 3 regions, i.e. the frontal association cortex, primary somatosensory cortex (lip, and jaw region), and primary motor cortex. The 2nd network involved 4 regions in the left hemisphere, i.e. the caudomedial and dorsolateral entorhinal cortex, parasubiculum, and perirhinal cortex. The 3rd network involved 25 regions, including the bilateral dorsal intermediate entorhinal cortex, posterolateral amygdaloid area, piriform cortex, hippocampus, amygdala, striatum, preoptic telencephalon, and anterior commissure. Interestingly, tracts involving interhemispheric connectivity such as the corpus callosum and sensory processes such as optic and olfactory tracts were identified as important as well, even if present just unilaterally. The visual cortex, accumbens, superior colliculus, medial geniculate, and septum were also part of this large subnetwork. The 4th component involved interhemispheric thalamic connectivity, including for the ventral thalamic nuclei. Among the remaining subnetworks we note the interhemispheric hypothalamic connections, primary and secondary somatosensory cortices, visual cortex, insula, ectorhinal cortex, as well as the superior colliculus and periaqueductal gray. Interestingly the gigantocellular reticular nuclei and tectospinal tract were also found

amongst the top 13 subnetworks. Thus, a wide range of functionally distinct regions differed in connectivity due to different APOE alleles carriage.

Age and APOE

We identified 239 edges that were common for the risk factors represented by age and APOE4 allele carriage versus APOE3 allele carriage. These constituted 12 subnetworks and the top 50 edges are shown **in Figure 4 B**. The top network involved 4 regions, i.e. the left frontal association cortex, left S1 (jaw, upper lip), and left M1. The 2nd subnetwork involved 24 regions, 7 bilateral nodes, 7 unique to the left hemisphere, and 3 unique to the right hemisphere. The nodes with bilateral presence included the lateral orbital cortex, the dorsal intermediate and the caudomedial entorhinal cortex, piriform, accumbens, lateral olfactory tract, and cerebellar cortex. The nodes present only in the left hemisphere included the insula, dorsolateral entorhinal cortex, S1, hippocampus, amygdala and striatum, anterior commissure, and cerebellar white matter; and the nodes only present in the right hemisphere included the right medial entorhinal cortex, anterior commissure and cerebellar white matter. The 3rd subnetwork included a bilateral hypothalamus and the left preoptic telencephalon. Among the remaining subnetworks we noted the presence of the temporal association cortex, septum, S2, M1, visual and auditory cortices, as well as the periaqueductal gray (bilateral), gigantocellular nucleus, and contralateral component of the hippocampus, striatum (right hemisphere), tectospinal tract and corpus callosum. While we recognized the presence of top subnetworks including regions responsible for APOE genotype differences, we also noted an additional cerebellar component.

Age Sex and Diet

We identified 197 edges that were common for the risk factors represented by age, sex and diet. These constituted 16 subnetworks and the top 50 edges are shown in **Figure 4 C**. The top subnetwork included 6 regions in the left hemisphere, i.e. the frontal association cortex, S1 (jaw), S2, M1, lateral orbital cortex, and insula. The 2nd subregion included 7 regions in the left hemisphere, i.e. caudomedial entorhinal and dorsolateral cortex, piriform, parasubiculum, amygdala, and posterolateral cortical amygdaloid nucleus, and the lateral olfactory tract. The 3rd network included the left hypothalamus and preoptic telencephalon. We noted the presence of septum and fimbria, thalamic nuclei, as well as the contralateral components for the majority of the components in the top

three subnetworks. Thus memory, sensory and motor components were identified as shared vulnerable subgraphs among the subgraphs associated with these three risk factors.

Common Edges

We identified 63 edges and 12 subnetworks that were common for risk factors including age, sex, APOE genotype, HN genotype, and diet. The top 50 edges are shown in **Figure 4D**. The top subnetwork included the left insula to lateral orbital cortex. The 2nd network included the left frontal association cortex, S1 (jaw) and M1. The 3rd network included the left caudomedial entorhinal cortex and parasubiculum. The other subgraphs included more components of the entorhinal cortex, septum, fimbria, temporal association areas, hypothalamus and preoptic telencephalon, as well as auditory cortex. The periaqueductal gray and superior colliculus were also present, as well as gigantocellular reticular nucleus. We have identified a small set of edges (0.11 % of the total 54946 edges in the mouse brain connectomes) that were common to all the risk factors.

3.5 Brain Networks with Distinct Vulnerability to Immune Perturbations

We examined genotype specific alterations of the connectome due to manipulation of the innate immune system. For the APOE2 versus APOE2HN comparison we obtained 265 HSP with upper bounds of 185 for false discoveries; for APOE3 versus APOE3HN we obtained 47 HSP with upper bounds of 3 for false discoveries; for APOE4 versus APOE4HN we obtained 1091 HSP with upper bounds 598 for false discoveries. The innate immune changes due to HN affected similar networks in different APOE genotypes and these changes affected memory networks, such as the entorhinal cortex for all genotypes. Other subnetworks affected in all three APOE genotypes included sensory areas such as the S2, the auditory cortex, motor areas, insula and cerebellum. We note that while APOE3 had almost neutral effects for connections within the entorhinal cortex, APOE2 mice had negative and APOE4 mice had positive weights associated with connections within the entorhinal cortex (black arrows in **Figure 5**) Caudal to Dorsal Entorhinal cortex). Upon examining the top 50 edges we noted that APOE2 mice spared the corpus callosum, APOE3 mice had changes in the corpus callosum, and APOE4 mice had changes specifically in the corpus callosum-hippocampus connectivity, bilaterally with a stronger weight for the left hemisphere.

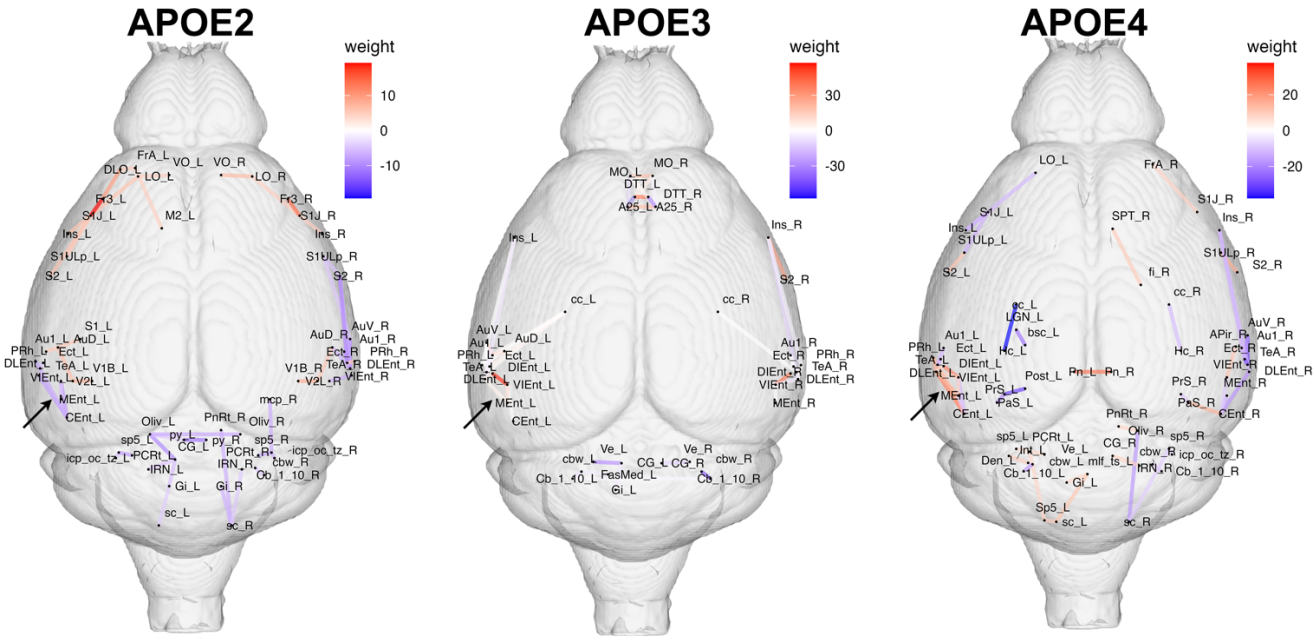

Figure 6. The innate immune changes due to HN affected similar networks in different APOE genotypes and these changes were located to memory networks, such as the entorhinal cortex. Other subnetworks affected included sensory areas such as the S2, the auditory cortex, motor areas, insula and cerebellum. We note that relative to the neutral APOE3 allele comparison, the connections within the entorhinal cortex (black arrows) in the APOE2 mice had negative weights, while in APOE4 mice they had positive weights (Caudal to Dorsal Entorhinal cortex).

3. Discussion

To understand the modifying effect of genetic and environmental risk factors for abnormal aging and Alzheimer's disease we have used mouse models with targeted replacement of the Apoe gene, expressing instead the human major APOE alleles: APOE2 which reduces risk, APOE3 which confers normal risk, and APOE4 which confers increased risk. We investigated separately the effects of age, sex, APOE genotype, and the humanized innate immune response modulation due to the human NOS2.

A global network analysis revealed that modifying the innate immune system by humanizing mNos2 was associated with changes in 6 parameters characterizing network topology, aging resulted in changes in 4 parameters, variations in APOE genotype in 1-3 parameters, and sex in 2 parameters. Diet, however, only

resulted in a p~0.1 for betweenness centrality and average clustering. The most frequent changes were observed in 3 out of 6 previously mentioned comparisons, for eigenvector centrality (denoting changes in nodes influence), betweenness centrality (level of nodes control over the network), average clustering coefficient (degree to which nodes tend to cluster), and shortest path length (related to efficiency of transfer of information). Two of the comparisons were significant for local efficiency, and the degree Pearson correlation or assortativity (related to the dependency of degrees for neighboring nodes). Together, these results support that immune system modifications results in strong differences in connectivity, information flow and network resilience; that age causes major network remodeling; and APOE genotype, and sex differences are also reflected in the architecture of brain networks.

To reveal local subgraphs vulnerable to individual risk factors, we sought high selection probability edges for each of them. The resulting networks were largely symmetrical, though weights appeared higher for the left hemisphere in general. When comparing connectomes for different APOE alleles, the most high selection probability edges were detected for APOE3 versus APOE4 (773 out of 54946, or 1.4 % of the total number of edges in the brain network), followed by 273 edges for the APOE2 versus APOE3 comparison, and 204 edges for the APOE2 versus APOE4 comparison. Thus, APOE2 mice were more similar to APOE4 mice in terms of their connectomes. These results concur with our previous behavioral investigation, which supported that APOE2 mice were more similar to APOE4 mice than to APOE3 mice in terms of their spatial navigation strategies (Badea, Li et al. 2022).

Connectome analyses revealed differences associated with age, sex, diet and HN carriage, and identified the largest number of edges for diet (1626), followed by sex, HN, and age. While it was not surprising to see a widespread effect of diet, we were surprised to see more edges for sex (~500) than for age (~300). This may be explained by the relatively small difference in age for our mice transitioning from middle to old age.

APOE based differences were stronger for the left hemisphere, but the contralateral regions were also present in a majority of cases, yielding highly symmetric subgraphs in general. APOE2 versus APOE3 differences involved the lateral orbital cortex, entorhinal and perirhinal cortex. Besides regions involved in executive function

and memory, the APOE3 versus APOE4 comparison emphasized the role of sensory and motor areas including vision (V1), taste, and pain (insula, periaqueductal gray). Sensory and motor associated regions have also been found to differ in asymptomatic APOE4 carriers relative to APOE3 carriers (Clarke, Messaritaki et al. 2022). We noted connectivity differences for the cerebellum, which has a well-known role in movement control but also in language processing, learning and memory (Koziol, Budding et al. 2014). Our results also support a role for the amygdala, involved in affective memory, and basal ganglia components.

As expected, age had a strong effect on association cortices (frontal and temporal), sensory and motor areas, and the olfactory tract, as well as basal ganglia and cerebellum. Our results in mouse models of aging agree in with human structural and functional connectomes, which are also influenced by aging in a number of regions (Madole, Ritchie et al. 2021).

There is growing interest into the mechanisms behind increased risk in older APOE4 females relative to males (Riedel, Thompson et al. 2016). Individual brain regions that have most consistently been reported as different in males and females include the basal ganglia, hippocampus, and amygdala (Lenroot and Giedd 2010). Sex differences revealed a role for memory related regions (entorhinal cortex, hippocampus), and surprisingly cerebellum. We also found septum and fimbria among relevant nodes. Differences in these structures (Yeung, Stolicyn et al. 2023) have been reported (Xin, Zhang et al. 2019). We also found differences in hypothalamus, a well-known sexually dimorphic region (Scott, Prigge et al. 2015). While less known as sexually dimorphic, the differences in the connectivity of gigantocellular (Anne, Flavio et al. 2020) nuclei support a possible change in locomotor recovery after injury (Sun, Wang et al. 2020).

Data on how AD risk is influenced by diet, and how a high fat diet affects particular brain networks (Franz, Xian et al. 2019). We identified using mouse models diet related connectivity differences in insula, which was shown to be one of the regions affected by diet (Rolls, Feng et al. 2023), together with other regions involved in attention (parahippocampal gyrus) and appetite control (Adise, Allgaier et al. 2021). Interestingly, we also noted a role for the hypothalamus for both diet and HN, and this has been shown to trigger inflammatory responses following a high fat diet, which in turn can lead to impaired synaptic plasticity, neurogenesis and neuromodulation (Mendes,

Kim et al. 2018). Our findings of diet associated brain changes in visual, auditory and cerebellar regions corroborate human studies that point to brain changes in specific areas, for example (Zeighami, Dadar et al. 2022) report diet associated changes in somatomotor, visual, and ventral attention areas, and propose changes in memory related areas as well (entorhinal cortex, and hippocampus). Our findings of common vulnerable networks for diet and aging, support studies showing that diet may affect brain aging (Shen, Liu et al. 2023).

The immune background caused significant alterations in the connectome, with a role for corpus callosum, piriform cortex and amygdala; and within genotype comparisons showed consistent involvement of the memory networks, as well as sensory components, in particular S2 and the auditory cortex. We detected the largest number of edges for APOE4, followed by APOE2 and then APOE3, suggesting increased sensitivity to innate immune system perturbations in the APOE4 genotype.

In our study we found graph edges common to age and APOE genotype, and these included the frontal association cortex, S1, and M1; as well as the lateral orbital cortex, entorhinal cortex and temporal association cortex. A study in human aging revealed that APOE4 carriers had an accelerated loss of structural connectivity in the inferior temporal gyrus, as well as the medial and lateral orbital cortex (Brown, Terashima et al. 2011).

We identified common edges for age sex and diet, and these included the entorhinal cortex, S1, S2, M1, lateral orbital cortex and insula, septum, amygdala and hypothalamus, fimbria and olfactory tract. These results concur in general to age related changes in the human functional connectome, and involve regions known to suffer greater cortical thinning in aging, such as those in the temporal lobe and sensory motor areas. Interestingly our mouse study identified the auditory cortex, while the human study identified the visual cortex, however this only accounted for aging but not sex and diet associated vulnerability.

Finally, we revealed overlaps in vulnerable brain network changes occurring in the whole set of risk factors included in our study, and these consisted of only 63 edges. Our results support a role for the orbitofrontal cortex, association cortices, S1 and M1, in addition to the memory related areas, e.g. entorhinal cortex septum, and their connections, e.g. the fimbria. Interestingly, S1, M1 and the auditory cortex were part of this small set,

underlying the importance of future studies on biomarkers for sensory motor markers for neurodegenerative diseases largely marked by cognition function loss, such as AD.

Our study has limitations inherent to the fact that mouse models do not fully replicate the complexity encountered in human populations, however these models provide a uniform genetic background and are raised in the same conditions; enabling smaller scale studies and interventions to be tested to reveal mechanistic insight into the etiology of disease and the ability to curbing its evolution, perhaps through lifestyle interventions such as dietary modification or exercise. Moreover, our study does not fully answer the question on the onset of connectome differences, thus more studies are necessary using younger animals.

4. Conclusion

Our connectome study compared APOE4 genotypes considered a high risk genotype in aging and AD to the neutral APOE3 genotypes to reveal vulnerable brain networks; as well as APOE2 as the protective genotype in aging and AD to the neutral APOE3 to reveal potentially resilient networks. By comparing mice with a different immune background, we discovered that it plays a large role and affects memory and sensory networks, but future studies should include more animals to assess genotype specific changes comparisons. Our overall results revealed vulnerable brain networks associated with multiple risk factors, including APOE genotype, sex, diet and innate immune response in mouse models of aging. These results provide insight into the reorganization of structural networks required to maintain functional status in cases of resilience to aging, or failing to do so during abnormal aging and AD. Further studies investigating the biological substrates may reveal metabolic and other omic changes associated with alterations in brain networks.

Data and Code availability: The connectome and associated metadata are available at https://zenodo.org/record/8377684. The code are publicly shared and the R package for visualization can be found at https://github.com/szwinter/MouseModels/ and we used visualization code from https://github.com/Ali-Mahzarnia/brainconn2.

Acknowledgments

This work was supported by RF1 AG057895, R01 AG066184, U24 CA220245, RF1 AG070149. We acknowledge support from the research staff in the Radiology department: Gary Cofer and Wyatt Austin, and BIAC staff: Chris Petty and Francis Favorini.

Supplementary Material

Supplementary Table 1. SAMBA Atlas Abbreviations

Supplementary Table 2: Subnetworks for risk factors

Supplementary Table3. Common Networks

REFERENCES

Adise, S., N. Allgaier, J. Laurent, S. Hahn, B. Chaarani, M. Owens, D. Yuan, P. Nyugen, S. Mackey, A. Potter and H. P. Garavan (2021). "Multimodal brain predictors of current weight and weight gain in children enrolled in the ABCD study ®." Developmental Cognitive Neuroscience **49**: 100948.

Anderson, R. J., N. Wang, J. J. Cook, G. P. Cofer, R. Dibb, G. A. Johnson and A. Badea (2018). "A high performance computing cluster implementation of compressed sensing reconstruction for MR histology." Proc. Intl. Soc. Mag. Reson. Med.

Anne, K. E., B. Flavio, P. S. Marc, P. Dario, I. Stefan, S. Regula, H. Anna-Sophie, W. Martin and E. S. Martin (2020). "The Gigantocellular Reticular Nucleus Plays a Significant Role in Locomotor Recovery after Incomplete Spinal Cord Injury." The Journal of Neuroscience **40**(43): 8292.

Arroyo Relión, J. D., D. Kessler, E. Levina and S. F. Taylor (2019). "NETWORK CLASSIFICATION WITH APPLICATIONS TO BRAIN CONNECTOMICS." Ann Appl Stat **13**(3): 1648-1677.

Badea, A., A. Kamnaksh, R. J. Anderson, E. Calabrese, J. B. Long and D. V. Agoston (2018). "Repeated mild blast exposure in young adult rats results in dynamic and persistent microstructural changes in the brain." NeuroImage: Clinical **18**: 60-73.

Badea, A., D. Li, A. Niculescu, R. Anderson, J. Stout, C. Williams, C. Colton, N. Maeda and D. Dunson (2022). Absolute Winding Number Differentiates Spatial Navigation Strategies with Genetic Risk for Alzheimer's Disease, bioRxiv.

Badea, A., K. L. Ng, R. J. Anderson, J. Zhang, M. I. Miller and R. J. O'Brien (2019). "Magnetic resonance imaging of mouse brain networks plasticity following motor learning." PLoS ONE **14**(5).

Brown, J. A., K. H. Terashima, A. C. Burggren, L. M. Ercoli, K. J. Miller, G. W. Small and S. Y. Bookheimer (2011). "Brain network local interconnectivity loss in aging APOE-4 allele carriers." Proceedings of the National Academy of Sciences of the United States of America **108**(51): 20760-20765.

Chuang, Y. F., Y. An, M. Bilgel, D. F. Wong, J. C. Troncoso, R. J. O'Brien, J. C. Breitner, L. Ferruci, S. M. Resnick and M. Thambisetty (2016). "Midlife adiposity predicts earlier onset of Alzheimer's dementia, neuropathology and presymptomatic cerebral amyloid accumulation." Mol Psychiatry **21**(7): 910-915.

Clarke, H., E. Messaritaki, S. I. Dimitriadis and C. Metzler-Baddeley (2022). "Dementia Risk Factors Modify Hubs but Leave Other Connectivity Measures Unchanged in Asymptomatic Individuals: A Graph Theoretical Analysis." Brain Connectivity **12**(1): 26-40.

Colton, C. A., M. P. Vitek, D. A. Wink, Q. Xu, V. Cantillana, M. L. Previti, W. E. Van Nostrand, J. B. Weinberg and H. Dawson (2006). "NO synthase 2 (NOS2) deletion promotes multiple pathologies in a mouse model of Alzheimer's disease." Proc Natl Acad Sci U S A **103**(34): 12867-12872.

Corder, E. H., A. M. Saunders, W. J. Strittmatter, D. E. Schmechel, P. C. Gaskell, G. W. Small, A. D. Roses, J. L. Haines and M. A. Pericak-Vance (1993). "Gene dose of apolipoprotein E type 4 allele and the risk of Alzheimer's disease in late onset families." Science **261**(5123): 921-923.

Dennis, N. A., J. N. Browndyke, J. Stokes, A. Need, J. R. Burke, K. A. Welsh-Bohmer and R. Cabeza (2010). "Temporal lobe functional activity and connectivity in young adult APOE ε4 carriers." Alzheimer's and Dementia **6**(4): 303-311.

Filippi, M., C. Cividini, S. Basaia, E. G. Spinelli, V. Castelnovo, M. Leocadi, E. Canu and F. Agosta (2023). "Age-related vulnerability of the human brain connectome." Molecular Psychiatry.

Hersi, M., B. Irvine, P. Gupta, J. Gomes, N. Birkett and D. Krewski (2017). "Risk factors associated with the onset and progression of Alzheimer's disease: A systematic review of the evidence." Neurotoxicology **61**: 143-187.

Hoos, M. D., M. P. Vitek, L. A. Ridnour, J. Wilson, M. Jansen, A. Everhart, D. A. Wink and C. A. Colton (2014). "The impact of human and mouse differences in NOS2 gene expression on the brain's redox and immune environment." Mol Neurodegener **9**: 50.

Kuceyeski, A. F., K. W. Jamison, J. P. Owen, A. Raj and P. Mukherjee (2019). "Longitudinal increases in structural connectome segregation and functional connectome integration are associated with better recovery after mild TBI." Human Brain Mapping **40**(15): 4441-4456.

Lenroot, R. K. and J. N. Giedd (2010). "Sex differences in the adolescent brain." Brain Cogn **72**(1): 46-55.

Liu, C. C., C. C. Liu, T. Kanekiyo, H. Xu and G. Bu (2013). "Apolipoprotein E and Alzheimer disease: risk, mechanisms and therapy." Nat Rev Neurol **9**(2): 106-118.

Madole, J. W., S. J. Ritchie, S. R. Cox, C. R. Buchanan, M. V. Hernández, S. M. Maniega, J. M. Wardlaw, M. A. Harris, M. E. Bastin, I. J. Deary and E. M. Tucker-Drob (2021). "Aging-Sensitive Networks Within the Human Structural Connectome Are Implicated in Late-Life Cognitive Declines." Biological Psychiatry **89**(8): 795-806.

Mahzarnia, A., J. A. Stout, R. J. Anderson, H. S. Moon, Z. Yar Han, K. Beck, J. N. Browndyke, D. B. Dunson, K. G. Johnson, R. J. O'Brien and A. Badea (2023). "Identifying vulnerable brain networks associated with Alzheimer's disease risk." Cerebral Cortex **33**(9): 5307-5322.

Mayeux, R., A. M. Saunders, S. Shea, S. Mirra, D. Evans, A. D. Roses, B. T. Hyman, B. Crain, M. X. Tang and C. H. Phelps (1998). "Utility of the apolipoprotein E genotype in the diagnosis of Alzheimer's disease. Alzheimer's Disease Centers Consortium on Apolipoprotein E and Alzheimer's Disease." N Engl J Med **338**(8): 506-511.

Mendes, N. F., Y.-B. Kim, L. A. Velloso and E. P. Araújo (2018). "Hypothalamic Microglial Activation in Obesity: A Mini-Review." Frontiers in Neuroscience **12**.

Mitra, J., K. K. Shen, S. Ghose, P. Bourgeat, J. Fripp, O. Salvado, K. Pannek, D. J. Taylor, J. L. Mathias and S. Rose (2016). "Statistical machine learning to identify traumatic brain injury (TBI) from structural disconnections of white matter networks." NeuroImage **129**: 247-259.

Riedel, B. C., P. M. Thompson and R. D. Brinton (2016). "Age, APOE and sex: Triad of risk of Alzheimer's disease." J Steroid Biochem Mol Biol **160**: 134-147.

Rolls, E. T., R. Feng and J. Feng (2023). "Lifestyle risks associated with brain functional connectivity and structure." Hum Brain Mapp **44**(6): 2479-2492.

Scott, N., M. Prigge, O. Yizhar and T. Kimchi (2015). "A sexually dimorphic hypothalamic circuit controls maternal care and oxytocin secretion." Nature **525**(7570): 519-522.

Shah, R. D. and R. J. Samworth (2013). "Variable Selection with Error Control: Another Look at Stability Selection." Journal of the Royal Statistical Society Series B: Statistical Methodology **75**(1): 55-80.

Singh-Manoux, A., A. Dugravot, M. Shipley, E. J. Brunner, A. Elbaz, S. Sabia and M. Kivimaki (2018). "Obesity trajectories and risk of dementia: 28 years of follow-up in the Whitehall II Study." Alzheimer's & Dementia **14**(2): 178-186.

Sun, P., J. Wang, M. Zhang, X. Duan, Y. Wei, F. Xu, Y. Ma and Y.-H. Zhang (2020). "Sex-Related Differential Whole-Brain Input Atlas of Locus Coeruleus Noradrenaline Neurons." Frontiers in Neural Circuits **14**.

Trachtenberg, A. J., N. Filippini, K. P. Ebmeier, S. M. Smith, F. Karpe and C. E. Mackay (2012). "The effects of APOE on the functional architecture of the resting brain." NeuroImage **59**(1): 565-572.

Valerio, Z., W. Maximilian, L. E. Tim, J. Diane, B. Maarten Van, P. C. M. Martina, F. B. Christian, H. Arend and J. K. Amanda (2014). "Resting-State Functional Connectivity Changes in Aging apoE4 and apoE-KO Mice." The Journal of Neuroscience **34**(42): 13963.

Veitch, D. P., M. W. Weiner, P. S. Aisen, L. A. Beckett, N. J. Cairns, R. C. Green, D. Harvey, C. R. Jack, W. Jagust, J. C. Morris, R. C. Petersen, A. J. Saykin, L. M. Shaw, A. W. Toga and J. Q. Trojanowski (2019). "Understanding disease progression and improving Alzheimer's disease clinical trials: Recent highlights from the Alzheimer's Disease Neuroimaging Initiative." Alzheimer's and Dementia **15**(1): 106-152.

Verhelst, H., C. Vander Linden, T. De Pauw, G. Vingerhoets and K. Caeyenberghs (2018). "Impaired rich club and increased local connectivity in children with traumatic brain injury: Local support for the rich?" Human Brain Mapping **39**(7): 2800-2811.

Wang, N., R. J. Anderson, A. Badea, G. Cofer, R. Dibb, Y. Qi and G. A. Johnson (2018). "Whole mouse brain structural connectomics using magnetic resonance histology." Brain Structure and Function **223**(9): 4323-4335.

Wang, X., A. L. Bey, B. M. Katz, A. Badea, N. Kim, L. K. David, L. J. Duffney, S. Kumar, S. D. Mague, S. W. Hulbert, N. Dutta, V. Hayrapetyan, C. Yu, E. Gaidis, S. Zhao, J. D. Ding, Q. Xu, L. Chung, R. M. Rodriguiz, F. Wang, R. J. Weinberg, W. C. Wetsel, K. Dzirasa, H. Yin and Y. H. Jiang (2016). "Altered mGluR5-Homer scaffolds and corticostriatal connectivity in a Shank3 complete knockout model of autism." Nature Communications **7**.

Ward, A., S. Crean, C. J. Mercaldi, J. M. Collins, D. Boyd, M. N. Cook and H. M. Arrighi (2012). "Prevalence of apolipoprotein E4 genotype and homozygotes (APOE e4/4) among patients diagnosed with Alzheimer's disease: a systematic review and meta-analysis." Neuroepidemiology **38**(1): 1-17.

Wiesmann, M., V. Zerbi, D. Jansen, R. Haast, D. Lütjohann, L. M. Broersen, A. Heerschap and A. J. Kiliaan (2016). "A Dietary Treatment Improves Cerebral Blood Flow and Brain Connectivity in Aging apoE4 Mice." Neural Plast **2016**: 6846721.

Xie, T. and Y. He (2012). "Mapping the alzheimer's brain with connectomics." Frontiers in Psychiatry **2**(JAN).

Xin, J., Y. Zhang, Y. Tang and Y. Yang (2019). "Brain Differences Between Men and Women: Evidence From Deep Learning." Front Neurosci **13**: 185.

Yeung, H. W., A. Stolicyn, C. R. Buchanan, E. M. Tucker-Drob, M. E. Bastin, S. Luz, A. M. McIntosh, H. C. Whalley, S. R. Cox and K. Smith (2023). "Predicting sex, age, general cognition and mental health with machine learning on brain structural connectomes." Hum Brain Mapp **44**(5): 1913-1933.

Zamani Esfahlani, F., J. Faskowitz, J. Slack, B. Mišić and R. F. Betzel (2022). "Local structure-function relationships in human brain networks across the lifespan." Nature Communications **13**(1): 2053.

Badea, A., W. Wu, J. Shuff, M. Wang, R. J. Anderson, Y. Qi, G. A. Johnson, J. G. Wilson, S. Koudoro, E. Garyfallidis, C. A. Colton and D. B. Dunson (2019). "Identifying Vulnerable Brain Networks in Mouse Models of Genetic Risk Factors for Late Onset Alzheimer's Disease." Frontiers in Neuroinformatics **13**.

Colton, C. A., M. P. Vitek, D. A. Wink, Q. Xu, V. Cantillana, M. L. Previti, W. E. Van Nostrand, B. Weinberg and H. Dawson (2006). "No synthase 2 (NOS2) deletion promotes multiple pathologies in a mouse model of Alzheimer's disease." Proceedings of the National Academy of Sciences of the United States of America **103**(34): 12867-12872.

Colton, C. A., D. M. Wilcock, D. A. Wink, J. Davis, W. E. Van Nostrand and M. P. Vitek (2008). "The effects of NOS2 gene deletion on mice expressing mutated human AβPP." Journal of Alzheimer's Disease **15**(4): 571-587.

Franz, C. E., H. Xian, D. Lew, S. N. Hatton, O. Puckett, N. Whitsel, A. Beck, A. M. Dale, B. Fang, C. Fennema-Notestine, R. L. Hauger, K. C. Jacobson, M. J. Lyons, C. A. Reynolds and W. S. Kremen (2019). "Body mass trajectories and cortical thickness in middle-aged men: a 42-year longitudinal study starting in young adulthood." Neurobiology of Aging **79**: 11-21.

Koziol, L. F., D. Budding, N. Andreasen, S. D'Arrigo, S. Bulgheroni, H. Imamizu, M. Ito, M. Manto, C. Marvel, K. Parker, G. Pezzulo, N. Ramnani, D. Riva, J. Schmahmann, L. Vandervert and T. Yamazaki (2014). "Consensus paper: The cerebellum's role in movement and cognition." Cerebellum **13**(1): 151-177.

Raber, J., Y. Huang and J. W. Ashford (2004). "ApoE genotype accounts for the vast majority of AD risk and AD pathology." Neurobiology of Aging **25**(5): 641-650.

Raber, J., D. Wong, M. Buttini, M. Orth, S. Bellosta, R. E. Pitas, R. W. Mahley and L. Mucke (1998). "Isoform-specific effects of human apolipoprotein E on brain function revealed in ApoE knockout mice: Increased susceptibility of females." Proceedings of the National Academy of Sciences of the United States of America **95**(18): 10914-10919.

Shen, C., C. Liu and A. Qiu (2023). "Metabolism-related brain morphology accelerates aging and predicts neurodegenerative diseases and stroke: a UK Biobank study." Translational Psychiatry **13**(1).

Sullivan, P. M., H. Mezdour, Y. Aratani, C. Knouff, J. Najib, R. L. Reddick, S. H. Quarfordt and N. Maeda (1997). "Targeted replacement of the mouse apolipoprotein E gene with the common human APOE3 allele enhances diet-induced hypercholesterolemia and atherosclerosis." Journal of Biological Chemistry **272**(29): 17972-17980.

TheAlzheimer'sAssociation (2023). The Patient Journey in the Era of New Treatments. https://www.alz.org/media/Documents/alzheimers-facts-and-figures.pdf. **2023 Alzheimer's Disease Facts and Figures**.

Xu, P. T., D. Schmechel, T. Rothrock-Christian, D. S. Burkhart, H. L. Qiu, B. Popko, P. Sullivan, N. Maeda, A. M. Saunders, A. D. Roses and J. R. Gilbert (1996). "Human apolipoprotein E2, E3, and E4 isoform-specific transgenic mice: Human-like pattern of glial and neuronal immunoreactivity in central nervous system not observed in wild-type mice." Neurobiology of Disease **3**(3): 229-245.

Zeighami, Y., M. Dadar, J. Daoust, M. Pelletier, L. Biertho, L. Bouvet-Bouchard, S. Fulton, A. Tchernof, A. Dagher, D. Richard, A. Evans and A. Michaud (2022). "Impact of weight loss on brain age: Improved brain health following bariatric surgery." NeuroImage **259**.